Optical Patternation of a Multi-hole Fuel Spray Nozzle

Jongmook Lim[1], Yudaya Sivathanu[2], Paul Sojka[3]

1. Jongmook Lim, En'Urga Inc., 1291A Cumberland Avenue, West Lafayette, IN 47906
2. Yudaya Sivathanu, En'Urga Inc., 1291A Cumberland Avenue, West Lafayette, IN 47906
3. Paul Sojka, School of Mechanical Engineering, Purdue University, West Lafayette, IN 47907

Patternation for a multi-hole spray nozzle using an extinction tomography based optical patternator is reported. Path integrated transmittances were obtained from a six-hole injector nozzle using water under cold flow conditions. The path-integrated transmittances were deconvoluted using the maximum likelihood estimation method with a new grid scheme. The current optical patternator uses only six view angle measurements because of limitation in the physical size of the instrument. However, a theoretical study with the new grid scheme showed that the angular resolution could be increased significantly by compromising radial resolution. Furthermore, an increase in angular resolution improves deconvolution error caused by the limited spatial resolution. The new technique was applied to measurements from a six hole injector nozzle and successfully resolved the droplet surface area spatial distribution.

1. Introduction

Patternation is the spatial distribution of mass or drop surface area perpendicular to the spray axis, measured at a fixed distance from the nozzle. It is important in a wide variety of applications. In gas turbine combustors, variations in the local spray mass can cause fuel rich or fuel lean pockets, leading to increased pollutant emissions. In automotive and furniture painting processes, poor finish quality can result from local variations in the mass of paints. Patternation of sprays is also important for numerical and theoretical model validation.

Bachalo [1] has recently reviewed the various diagnostic methods available to characterize spray nozzles. The two most popular methods used for spray characterization are particle sizing using Fraunhofer diffraction [2] and combined drop size and velocity determination using Phase Doppler Anemometry [3]. Black *et al*. [4] have reviewed the utilization of velocity and particle sizing measurements in industrial environments. However, patternation of sprays using these single point techniques is time consuming. Therefore, optical imaging is the preferred method for patternation of sprays.

Optical imaging has been widely used to characterize the local liquid concentrations in sprays [5]. The primary methods of optical imaging include high speed photography [6], holography [7], laser sheet imaging [8,9], and Planar Laser Induced Fluorescence imaging [10,11]. Imaging techniques that use either scattering or fluorescence to obtain patternation are suitable only for dilute sprays [12]. Two main difficulties in scattering and fluorescence techniques are the extinction of the light intensity by the intervening droplets and multiple scattering effects.

Corrections for the attenuation of light intensity [13] provide reasonable results for dilute sprays, since self-absorption in dilute sprays is small. In dense sprays, however, self-absorption of the scattered or fluoresced light is very high. No reliable method to correct for this self-absorption of the signal by the fluctuating flow field has been developed. Furthermore, no method is available to correct multiple scattering effects in dense sprays [17].

Recently, En'Urga Inc. developed a statistical extinction based patternator [14]. The SETscan patternator obtains the surface area of drops per unit volume [15] from path integrated extinction measurements. Deconvolution of the extinction measurements is based on the Maximum Likelihood Estimation (MLE) method [16]. Utilization of extinction tomography implies that the patternator can be used for both dilute and dense sprays [17]. Furthermore, the local extinction coefficient is directly proportional to the surface area of drops per unit volume [15].

Multi-hole injectors are commonly used in gas turbine engines to achieve wider and more uniform distribution of the spray. The importance of characterization of the spray pattern for the multi-hole injectors is more critical than for single hole injector because of possibility of non uniformity in the spatial distribution is much higher. Since the SETscan only takes six view angle measurements because of limitations in the physical size and number of optical elements, it is a challenge to resolve the spatial pattern of multi-hole spray injectors with the limited view angle measurements. Because of this, the objective of the present study was to evaluate the feasibility of resolving spray patterns from multi-hole injectors using a new grid scheme.

2. Experimental Methods

Path integrated transmittances were measured for six view angles, using 256 parallel paths for each view angle. The measurements were obtained using a 6-axes patternator (SETScan, Model OP600, En'Urga Inc.). A photograph of the patternator is shown in Fig. 1.

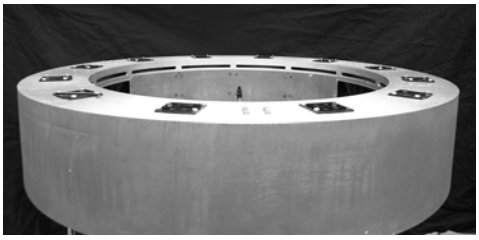

Figure 1. Photograph of the SETscan patternator.

A spray nozzle with six holes was mounted on top of the patternator as shown in Fig. 2. Alignment of the injector axis to the center of the patternator is not crucial. Therefore, the spray was mounted directly onto a swivel arm as shown in Fig. 2. The six-hole injector was driven using a water pump. The spray was run at steady state for 15 seconds. Path integrated transmittance was obtained at 1000 Hz and the data averaged to obtain the mean transmittances. The extinction measurements were converted to local extinction coefficients using statistical deconvolution [14,15]. The local extinction coefficient is identically equal to the local surface area per unit volume within the spray.

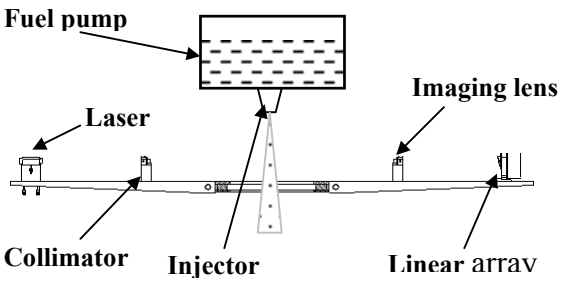

Figure 2. Schematic of the experimental arrangement.

One issue is the angular resolution of the measurements. There are six view angles possible for obtaining path-integrated transmittance data. However, at each view angle it is possible to obtain a very high number of parallel path transmittance measurements. Therefore a new grid scheme, as described below, was used to increase angular resolution by compromising radial resolution.

3. Theoretical Methods

The SETScan patternator provides measurements for only six view angles so the angular resolution is only 30 degrees and not sufficient to resolve the spatial distribution of the drop surface areas. However, the radial resolution of approximately 0.5 mm is more than sufficient to resolve the spatial distribution of drop surface areas. One possible method of increasing the angular resolution is to sacrifice some radial resolution by employing a novel grid scheme.
A conventional grid scheme for a patternator that obtains eight parallel path integrated transmittance measurements over six view angles is shown in Fig. 3.

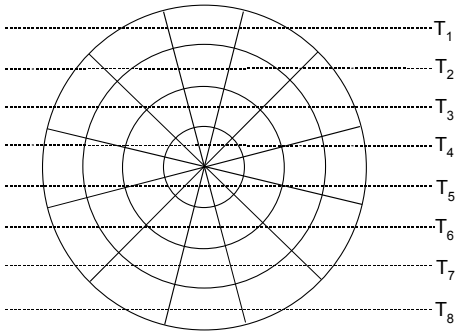

Figure 3. A conventional grid scheme with 30-degree angular resolution.

The measurement domain is divided into 4 radial and 12 angular segments, providing an angular resolution of 30 degrees. In each segment the extinction coefficients are assumed to be homogeneous. A total of 48 measurements are obtained from measurements over the six view angles. The number of unknown extinction coefficients within the segments in the domain is 48 (= 4 x 12), which is equal to the number of measurements (6 x 8). Therefore, a unique solution for the local extinction coefficients can be obtained. This is the conventional grid system.

The new grid scheme used in this study increases the angular resolution by reducing the number of radial grids. This new grid scheme is shown in Fig. 4.

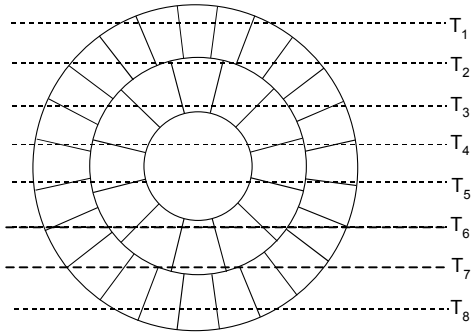

Figure 4. The new grid scheme with 15-degree angular resolution.

The measurement domain is divided into three radial segments, with different angular segments for each of the three radial segments. A total of 24 angular segments are provided for the outermost radial segment, 12 angular segments for the middle radial segment, and one angular segment for the innermost radial segment. Therefore, the angular resolution at the outermost segment is 15 degrees, which is twice that obtained with the conventional grid scheme. The radial segments are reduced from 4 to 3 for the same eight parallel path measurements. The center segment does not have an angular grid in order to make the system less sensitive to noise. Since the total number of segments is 37 and the available measurements are 48, the extinction coefficients for all segments can be found using the MLE method [15].

One important issue in the development of the new grid scheme is linear independence of the measurements. If two measurements (lines of sight) pass through the same grids, the measurements are linearly dependent. In this case, they essentially have the same information. All the measurements in Fig. 4 (T_1 – T_8) pass through different segments, and therefore are linearly independent. An addition benefit of the grid scheme shown in Fig. 4 is that the area within each grid is more uniform. The areas of segments in Fig. 3 are smallest at the center and largest at the outer ring. In general, any non-uniformity in the segments leads to a higher sensitivity of the solution to the measurement noise.

The performance of the new grid scheme was first evaluated using synthetic data. A contour plot of the local extinction coefficients used for creating the synthetic path integrated transmittances is shown in Fig. 5.

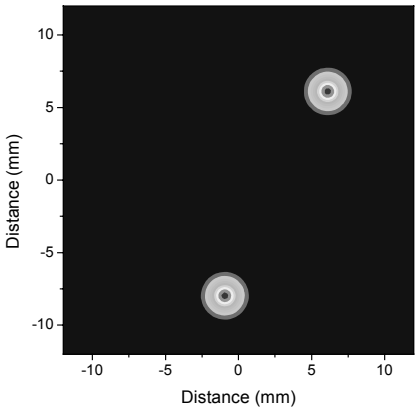

Figure 5. Contour plot of the local extinction coefficients used for the synthetic data.

The deconvolution domain is circular and its diameter is 24 mm. The number of parallel paths for one view angle was taken to be 256 (identical to the SETScan optical patternator). There are two dense spots in the domain and their diameters are 4.6 mm. A clipped Gaussian function (ensuring a smooth profile), as shown below, was used.

$$f(r) = \frac{1}{\sigma R\sqrt{2\pi}} \exp(-\left[(r/\sigma R)^2\right]/2) \tag{1}$$

Here R is a radius of the dense spot, and r the radial coordinate. The variance is given as σ=1/3. The peak extinction coefficient at the center of the dense spot is 0.11 mm^{-1}.

The synthetic local extinction coefficients were used to calculate path integrated transmittances. The deconvolution algorithm was then used with these path integrated transmittances to recover the local extinction coefficients. Both the conventional and new grid schemes were used. Deconvolution was first attempted with the conventional grid scheme. This scheme used 12 angular and 128 radial grids. The local extinction coefficients are shown in Fig. 6 (a).

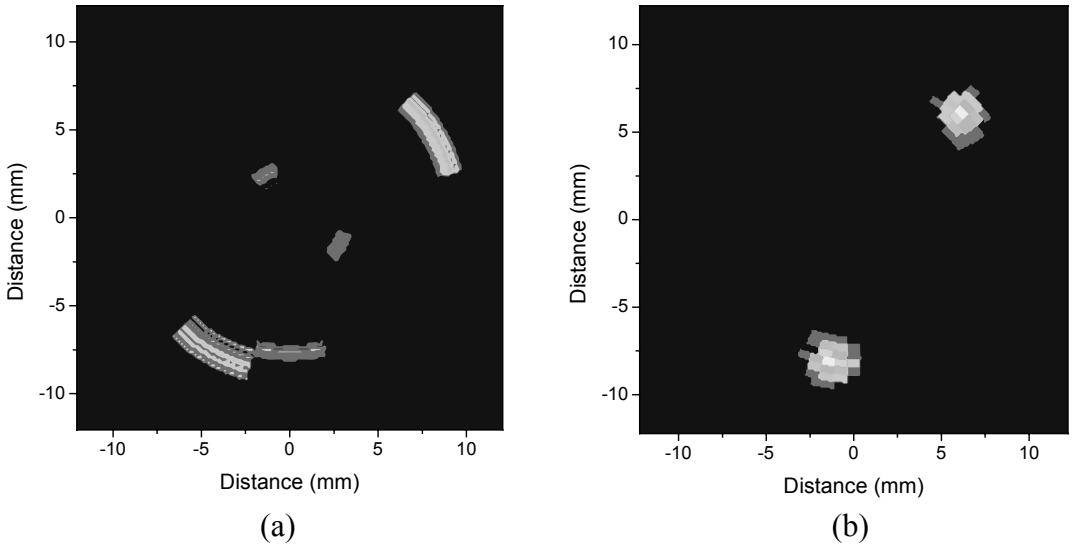

Figure 6. Deconvoluted local extinction coefficient using different grid schemes.

The peak values coefficients are 0.07, approximately 40% lower than the value that was used in creating the synthetic data, and are elongated in the circumferential direction because of low angular resolution. In addition, some noise is visible near the center of the domain. Therefore, it is evident that the lower angular resolution results in a smearing of the local extinction coefficients.

The same data set was used with the new grid scheme, consisting of 96 outermost angular grids and 29 radial grids. The local extinction coefficients obtained with the new grid scheme are shown in Fig. 6(b). The two dense spots in Fig. 6(b) are very close to the circular shape of the original pattern while the peak extinction coefficient is 0.091 (approximately 85 % of the synthetic data value). A quantitative method of studying the effect of changing the angular resolution is to examine the RMS fitting error. The RMS of fitting error is defined as

$$Err = \sqrt{\sum_{i=0}^{N} \left(\tau_{syn}^{i} - \tau_{dec}^{i}\right)^2 / N} \qquad (2)$$

where τ_{syn}^{i} is the synthetic path integrated transmittance for optical path i, and τ_{syn}^{i} is the deconvoluted path integrated transmittance.

The RMS fitting error as a function of the number of outermost angular grids is shown in Fig. 7.

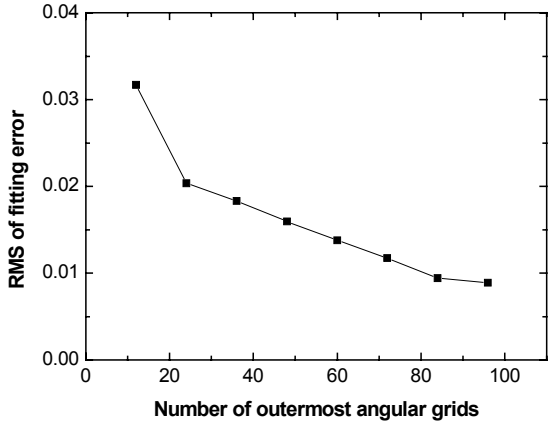

Figure 7. Fitting error with respect to the number of outermost angular grids.

The RMS error decreases by a factor of 3 when the angular resolution increases from 30 to 3.75 degree. In addition, the area of each segment is more uniform with different angular resolutions at different radial locations.

4. Experimental Results and Discussion

The new grid scheme was applied to measurements obtained using the SETScan optical patternator. The path-integrated transmittances measured using the patternator for a six hole spray are shown in Fig. 8. The measurements are shown as symbols in Fig. 8.

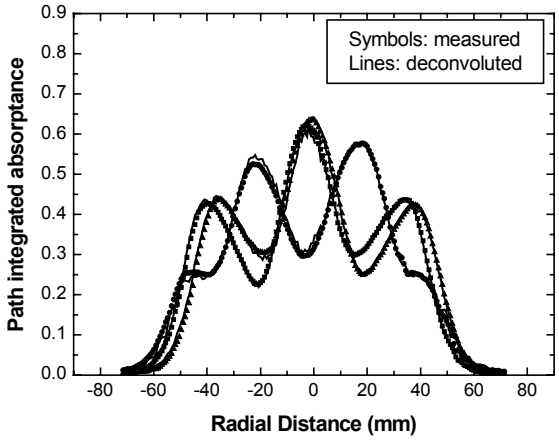

Figure 8. Path-integrated absorptance measurements for all six axes.

The absorptance profiles have three peaks because the spray nozzle has six holes. The effects of self-absorption and multiple scattering are significant for this spray, especially at locations with high absorptances. Therefore, other methods of optical patternation, such as laser sheeting imaging, or Planar Laser Induced Fluorescence, cannot be used [17]. The only reliable method of obtaining patternation for this nozzle is to use extinction tomography [17]

The path integrated measurements were deconvoluted using a grid having 96 angular segments in the outermost ring, and 17 radial rings with a progressively smaller number of angular segments. The path-integrated transmittances obtained at the point of convergence from the deconvolution algorithm is shown as lines. The measured and deconvoluted path integrated absorptances are in excellent agreement for all six axes.

The RMS fitting error for all six axes is less than 0.010. This low fitting error indicates that the distribution of surface area for six hole injector is sufficiently resolved. A contour plot of the local drop surface area per unit volume is shown in Fig. 9(a).

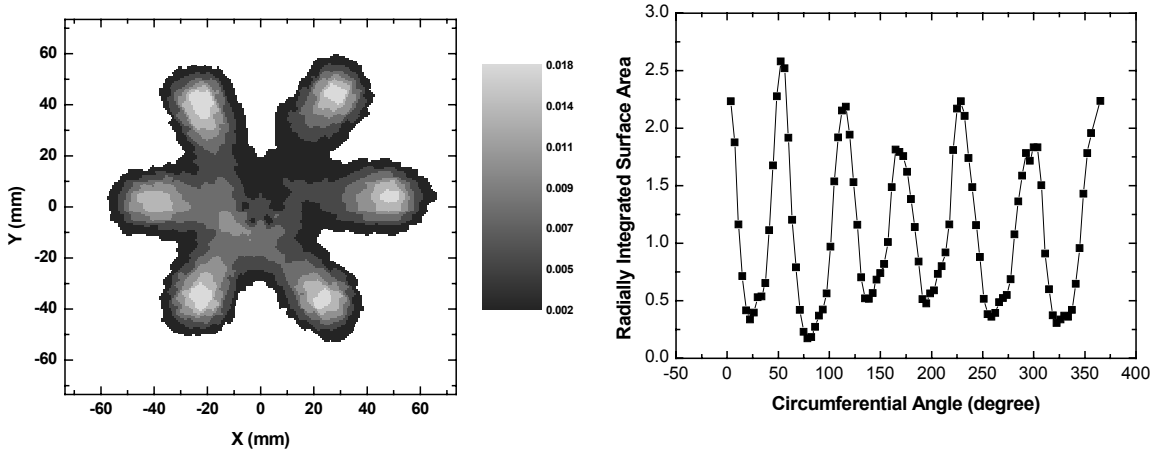

(a) (b)

Figure 9. Contour and patternation results for the injector six-hole injector.

Jets formed by the six-holes in the injector are clearly visible and slightly asymmetrical. A few red spots indicate dripping of the water spray. The patternation number can be obtained by integrating the local drop surface area per unit volume within a pie [15]. The local drop surface area per unit volume integrated over the radius is shown in Fig. 9(b). There are six local peaks, with each peak corresponding to one of the six injector holes. The asymmetry in the surface area distribution is evident from the Fig. 9(b). This data is extremely useful in quickly estimating the quality of the nozzle.

5. Conclusions

The following conclusions were obtained from the present study.

1. The angular resolution of measurements obtained using extinction tomography can be significantly improved by using the new grid scheme.

2. The deconvolution error is lower when a higher angular resolution is used at the outermost radial locations.
3. The spatial distribution of droplet surface area produced by a six-hole injector nozzle was successfully resolved using the six-axis optical patternator.

6. Acknowledgement

The optical patternator described in this study was developed under a National Science Foundation SBIR grant, with Dr. Jean Bonney serving as the NSF Program Officer. Useful technical discussions with Mr. Vinoo Narayanan and Ms. Seungmin Chang are also acknowledged.

7. References

[1] Bachalo W D 2000 *Atomization and Spray.* **10** 439-474.
[2] Swithenbank J 1976 *AIAA Paper*, 76-79.
[3] Farmer W M 1972 *Appl. Opt.* **11** 2603-2612.
[4] Black D L, McQuay M Q and Bonin M P 1996 *Prog. Energy Combust. Sci.* **22** 267-306.
[5] Chigier N 1991 *Prog. Energy Combust. Sci.* **17** 211-262.
[6] Chella G, Tognotti N L and Zamelli S 1986 *Atomization Spray Technol.* **2** 187-200.
[7] Wuerer J E, Oeding R G, Poon C C and Hess C F 1982 *AIAA Paper* 82-2336.
[8] Sankar S V, Robart D M, Maher K E, Mayo W T and Bachalo W D 1997 *Proceedings of ILASS Americas '97,* Ottawa, Canada, 266-271.
[9] Talley D G, Lin Y C and Morris M 1991 *Atomization and Spray.* **1**, 89-112.
[10] Melton L A and Verdieck J F 1985 *Combust. Sci Tech.* **42**, 217-22.
[11] Talley D G, Thamban A T S, McDonell V G, and Samuelsen G S 1995 *Progress in Astronautics and Aeronautics*. **166**, 113-141.
[12] Ruff G A and Faeth G M 1995 *Progress in Astronautics and Aeronautics*. **166**, 263-296.
[13] Talley D and Verdieck J 1996 *Proceedings of ILASS Americas '96,* San Fransicco, CA, 33-37.
[14] Sivathanu Y R, Lim J and Joseph R K *J. Quant. Spectrosc. Radiative Transfer.* **68**, 611-623.
[15] Lim J, Sivathanu Y, Narayanan V and Chang S 2003 *Atomization and Sprays,* **13**, 27-43.
[16] Vardi Y and Lee D 1993 *J. R. Statist. Soc. B*, **55**, 569-612.
[17] Brown C T, McDonell V G and Talley D G 2002, *Proceedings of ILASS Americas '00,* Madison, Wisconsin, 195-199.